ELSEVIER

Journal of Organometallic Chemistry 640 (2001) 182–196

Journal of Organo metallic Chemistry

www.elsevier.com/locate/jorganchem

Selectivity for the methoxycarbonylation of ethylene versus CO–ethylene copolymerization with catalysts based on C_4-bridged bidentate phosphines and phospholes

Simon Doherty [a,*], Edward G. Robins [a], Julian G. Knight [b,*], Colin R. Newman [b], Barrie Rhodes [b], Paul A. Champkin [b], William Clegg [b]

[a] *School of Chemistry, David Keir Building, The Queen's University of Belfast, Stranmillis Road, Belfast BT4 5AG, UK*
[b] *Department of Chemistry, Bedson Building, The University of Newcastle upon Tyne, Newcastle upon Tyne NE1 7RU, UK*

Received 4 July 2001; accepted 2 August 2001

Abstract

The C_4-bridged phospholes 11,12-bis(2,3,4,5-tetramethylphospholylmethyl)-9,10-dihydro-9,10-ethano-anthracene (*cis*, **4a**; *trans*, **4b**) and diphosphines 11,12-bis(diphenylphosphinomethyl)-9,10-dihydro-9,10-ethano-anthracene (*cis*, **5a**; *trans*, **5b**) and their corresponding palladium complexes [(P–P)$PdCl_2$] (**6a**–**d**) have been prepared and characterized. Single-crystal X-ray analyses of **6a**–**d** have been undertaken and they reveal that **4a** and **b** and **5a** and **b** coordinate in a bidentate manner forming seven-membered chelate rings with natural bite angles between 98.62 and 100.30°. The palladium-catalyzed carbonylation of ethylene has been studied using **4a** and **b** and **5a** and **b**. Catalyst mixtures generated from **4a** and **b**, palladium acetate and methanesulfonic acid are selective for the copolymerization of ethylene with carbon monoxide, generating low molecular weight polymers. Surprisingly, the activity of catalyst systems based on *cis*-(**4a**) is markedly higher than that based on its *trans*-isomer, **4b**. The marked influence of the nature of the four-carbon tether is highlighted by comparative catalyst testing with [{1,4-bis(2,3,4,5-tetramethylphospholyl)butane}$Pd(OAc)_2$], which rapidly decomposes under the conditions used for copolymerization. In contrast, under identical conditions catalyst mixtures formed from **5a** and **b** show a marked dependence of the selectivity on the stereochemistry of the ethano-anthracene tether, the former generating a low molecular weight copolymer while the latter generate mainly methyl propanoate. Interestingly, polyketone generated from catalysts based on bisphosphole **4a** has a markedly higher average molecular weight than that formed using its diphenylphosphino counterpart, **5a**.

Keywords: Diphosphines; Copolymerization; Ethylene; Carbon monoxide; Methoxycarbonylation; Selectivity

---

1. Introduction

The palladium-catalyzed carbonylation of unsaturated substrates such as alkenes and alkynes is a powerful tool in organic synthesis and has been used to prepare a range of important compounds [1]. For instance, intramolecular versions of this reaction have been used to synthesize five- and six-membered γ-lactones from the corresponding yne–ol [2]; enantioselective hydroxycarbonylation has been used to prepare α-aryl propionic acid derivatives [3], precursors to non-steroidal anti-inflammatory drugs, and alkoxycarbonylation has been used to synthesize oxygenated terpene derivatives, which find commercial applications in flavoring compositions and perfumes [4]. When the substrate is ethylene and the reaction medium methanol, palladium-catalyzed carbonylation results either in the alternating copolymerization of carbon monoxide and ethylene, to generate polyketone, or methoxycarbonylation to give methyl propanoate (Eq. (1)). The alternating copolymerization of olefins with carbon monoxide has attracted interest because of the useful properties of polyketone, which has been heralded as a new engineering thermoplastic, a tough,

---

* Corresponding authors. Fax: +44-28-90665297 (S.D.); +44-191-2226929 (J.G.K.).

E-mail addresses: s.doherty@qub.ac.uk (S. Doherty), j.g.knight@newcastle.ac.uk (J.G. Knight).

PII: S0022-328X(01)01180-9

flexible, wear-resistant, high impact strength polymer which has been developed into commercial products [5], while methyl propanoate is a potential intermediate in the manufacture of acrylic esters, large volume chemical intermediates which are produced annually on a multi-million tonne scale [6].

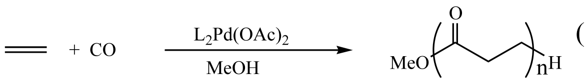

(1)

Since the initial discovery that catalysts based on palladium acetate and a bidentate phosphine were highly active and selective for copolymerization, selectivity has commonly been believed to be determined by ligand denticity, catalysts based on bidentate phosphines giving high molecular weight copolymer and those based on monodentate phosphines giving methyl propanoate. Indeed, a range of systems based on a palladium or nickel precursor and a bidentate phosphorus or nitrogen donor have been shown to catalyze the copolymerization of α-olefins with carbon monoxide [7]. However, in a recent study, workers at INEOS Acrylics discovered that the bidentate phosphine 1,2-bis(di-*tert*-butylphosphinomethyl)benzene in combination with $Pd_2(dba)_3$ forms a catalyst mixture that is exceptionally active (440 000 g product (mol cat)$^{-1}$ h^{-1}) and highly selective (99.98%) for methyl propanoate production [8]. Heaton and co-workers have used a combination of multinuclear NMR spectroscopy and ^{13}C-labeling to show that methoxycarbonylation of ethene most likely occurs via a hydride rather than the alternative methoxycarbonyl cycle [9]. Further evidence in support of the hydride mechanism has been provided by the isolation and characterization of the 3-oxopentyltriphenylphosphine cation, a by-product formed during the catalytic methoxycarbonylation of ethene [10], and the isolation of palladium-hydride and -acyl complexes, key intermediates in the catalytic hydroesterification of styrene [11]. In contrast, we have recently found that catalyst mixtures based on the *o*-xylyl-tethered bidentate phosphole, 1,2-bis(2,3,4,5-tetramethylphospholylmethyl)-benzene, are highly active and selective for the production of polyketone, demonstrating that replacement of di-*tert*-butyl groups for the 2,3,4,5-tetramethylphospholyl fragment affects a dramatic change in selectivity [12]. The disparate selectivity of these two catalyst systems, both containing an *o*-xylyl tether, suggests that the origin of selectivity in the palladium-catalyzed carboxylation of ethylene may not depend solely on monodentate versus bidentate coordination.

In an extension of our preliminary studies, we have investigated the potential of related C_4-bridged diphosphines to catalyze the carboxylation of ethylene and found that those based on *cis*- and *trans*-1,2-bis-(diphenylphosphinomethyl)cyclohexane and *endo*, *endo*-2,3-bis(diphenylphosphinomethyl)norbornane derivatives are selective for the production of copolymer while that based on *endo*, *exo*-2,3-bis(diphenylphosphinomethyl)norbornane is selective for methyl propanoate [13]. Herein, we report that the bidentate phospholes *cis*- and *trans*-11,12-bis(2,3,4,5-tetramethylphospholylmethyl)-9,10-dihydro-9,10-ethano-anthracene form catalysts that are selective for copolymer whereas the selectivity of their diphenylphosphino counterparts depends on the stereochemistry of the anthracene tether, catalysts based on *trans*-11,12-bis(diphenylphosphinomethyl)-9,10-dihydro-9,10-ethano-anthracene giving mainly methyl propanoate while *cis*-11,12-bis-(diphenylphosphinomethyl)-9,10-dihydro-9,10-ethano-anthracene is selective for polyketone.

2. Experimental

2.1. General comments

All manipulations involving air-sensitive materials were carried out in an inert atmosphere glove box or using standard Schlenk line techniques under an atmosphere of nitrogen or argon. Diethyl ether and hexane were distilled from potassium–sodium alloy, THF from potassium, and CH_2Cl_2 and pyridine from CaH_2. Deuteriochloroform was pre-dried with CaH_2, and then vacuum transferred and stored over 4 Å molecular sieves. 1,1,1,3,3,3-Hexafluoropropan-2-ol was purchased from Aldrich and used as received. ^{1}H-, ^{31}P- and ^{13}C-NMR spectra were recorded in JEOL LAMBDA 500 or Bruker AC 200, AMX 300 and DRX 500 machines. Gas chromatographic analysis was carried out using a Pye Unicam Series 104 instrument using the following conditions: initial temperature 50 °C for 2 min, final temperature 150 °C, ramp rate 12 °C min^{-1}, injection temperature 200 °C, detector temperature 200 °C, carrier gas N_2 55 ml min^{-1}, column: 2 m × 4 mm id, 20% Carbowax 20M on Gas-Chem Q 85-100 mesh. The diphosphines *cis*- and *trans*-{11,12-bis(2,3,4,5-tetramethylphospholylmethyl)-9,10-dihydro-9,10-ethano-anthracene} (**4a** and **b**) and 11,12-bis-(diphenylphosphinomethyl)-9,10-dihydro-9,10-ethano-anthracene (**5a** and **b**) were prepared from the corresponding dimesylates [14] as described below. 1-Phenyl-2,3,4,5-tetramethyl phosphole was prepared according to a previously published method [15].

2.1.1. Synthesis of 9,10-dihydro-9,10-ethano-anthracene-11,12-dicarboxylic acid-anhydride (**1a**)

Anhydrous aluminum chloride (41.14 g, 309 mmol) was added portion-wise to a suspension of anthracene (50.0 g, 281 mmol) in CH_2Cl_2 (500 ml) and cooled to 0 °C. A CH_2Cl_2 solution of maleic anhydride (27.51 g, 281 mmol) was added in portions to maintain the reaction mixture at 0 °C. After warming to room temperature (r.t.) and stirring overnight, the suspension was carefully poured onto water (750 ml), the organic layer separated, and the aqueous layer extracted with CH_2Cl_2 (3 × 75 ml). The organic extracts were combined, washed with water (200 ml), dried over $MgSO_4$ and the solvent removed to afford the desired anhydride, **1a**, as a tan solid in 87% yield (67.67 g). ^{1}H-NMR (500.0 MHz, $CDCl_3$, δ): 7.32 (dd, 2H, $J_{HH} = 3.4$, 6.8 Hz, C_6H_4), 7.26 (dd, 2H, $J_{HH} = 3.6$, 6.7 Hz, C_6H_4), 7.12 (m, 4H, C_6H_4), 4.76 (s, 2H, bridgehead C–*H*), 3.45 (s, 2H, ethano bridge C-*H*). $^{13}C\{^1H\}$-NMR (125.65 MHz, $CDCl_3$, δ): 170.4 (s, *C*O), 140.6 (s, C_6H_4), 138.0 (s, C_6H_4), 127.7 (s, C_6H_4), 127.1 (s, C_6H_4), 125.2 (s, C_6H_4), 124.3 (s, C_6H_4).

2.1.2. Synthesis of trans-9,10-dihydro-9,10-ethano-anthracene-dicarboxylic acid-(11,12)-diethyl ester (1b)

trans-9,10-Dihydro-9,10-ethano-anthracene-dicarboxylic acid-(11,12)-diethyl ester (**1b**) was prepared from diethyl fumarate and isolated in 82% yield according to the procedure described above for **1a**. ^{1}H-NMR (500.0 MHz, $CDCl_3$, δ): 7.00–7.28 (m, 8H, C_6H_4), 4.65 (s, 2H, bridgehead C–*H*), 3.99 (m, 4H, CH_2), 3.34 (s, 2H, ethano bridge C–*H*), 1.14 (t, 6H, $J_{HH} = 7.2$ Hz, CH_3).

2.1.3. Synthesis of cis-11,12-bis(hydroxymethyl)-9,10-dihydro-9,10-ethano-anthracene (2a)

A solution of **1a** (36.47 g, 132 mmol) in THF (100 ml) was added dropwise via cannula to a stirred suspension of lithium aluminum hydride (20.0 g, 527 mmol) in THF (300 ml) at 0 °C. After the addition was complete, the mixture was heated at reflux overnight. After cooling to r.t., the suspension was diluted with THF (600 ml) and quenched by addition of water (20 ml), followed by NaOH (8.0 g in 20 ml of water) and finally water (20 ml). After hydrolysis was complete, the resulting mixture was filtered, the solids washed with THF (3 × 100 ml) and the solvent removed in vacuo. Crystallization of the crude product from EtOH at r.t. yielded diol **2a** in 61% yield (21.5 g). ^{1}H-NMR (200.1 MHz, $CDCl_3$, δ): 6.97–7.24 (m, 8H, C_6H_4), 4.13 (s, 2H, bridgehead C–*H*), 3.44 (dd, 2H, CH_2OH), 3.22 (dd, 2H, CH_2OH), 2.74 (br s, 2H, CH_2OH), 2.26 (m, 2H, ethano bridge C–*H*).

2.1.4. Synthesis of trans-11,12-bis(hydroxymethyl)-9,10-dihydro-9,10-ethano-anthracene (2b)

trans-11,12-Bis-(hydroxymethyl)-9,10-dihydro-9,10-ethano-anthracene was isolated in 78% yield according to the procedure described above for **2a**. ^{1}H-NMR (500 MHz, $CDCl_3$, δ): 7.90 (dd, 2H, $J_{HH} = 3.3$, 6.4 Hz, C_6H_4), 7.40 (dd, 2H, $J_{HH} = 3.0$, 6.4 Hz, C_6H_4), 4.16 (s, 2H, bridgehead C–*H*), 3.41 (dd, 2H, $J_{HH} = 6.4$, 3.6 Hz, CH_2), 3.02 (dd, 2H, $J_{HH} = 2.8$, 7.9 Hz, CH_2), 2.0 (br s, 2H, CH_2OH), 1.66 (m, 2H, ethano bridge C–*H*). $^{13}C\{^1H\}$-NMR (125.65 MHz, $CDCl_3$, δ): 143.0–123.4 (C_6H_4), 66.3 (s), 46.4(s), 46.1 (s).

2.1.5. Synthesis of cis-11,12-bis(methanesulfonylmethyl)-9,10-dihydro-9,10-ethano-anthracene (3a)

Methanesulfonyl chloride (13.71 g, 119.7 mmol) was added to a stirred solution of **2a** (13.06 g, 49.0 mmol) in dry pyridine (130 ml) at such a rate to maintain the temperature below 5 °C. After stirring for further 1 h, the dark suspension was poured onto 1000 ml of 2 N HCl and stirred for 10 min. The solid was collected by filtration, washed with water (3 × 50 ml) and recrystallized from MeOH to give mesylate **3a** in 67% yield (13.8 g). ^{1}H-NMR (500.0 MHz, $CDCl_3$, δ): 7.27 (dd, 2H, $J_{HH} = 3.3$, 6.1 Hz, C_6H_4), 7.24 (dd, 2H, $J_{HH} = 3.3$, 6.1 Hz, C_6H_4), 7.1 (dd, 2H, $J_{HH} = 3.0$, 5.1 Hz, C_6H_4), 7.07 (dd, 2H, $J_{HH} = 3.3$, 4.7 Hz, C_6H_4), 4.33 (s, 2H, bridgehead C–*H*), 3.92 (dd, 2H, $J_{HH} = 5.5$, 10.0 Hz, CH_2), 3.65 (dd, 2H, $J_{HH} = 10.0$ Hz, CH_2), 2.87 (s, 6H, CH_3SO_3), 2.44 (br s, 2H, ethano bridge C–*H*).

2.1.6. Synthesis of trans-11,12-bis(methanesulfonylmethyl)-9,10-dihydro-9,10-ethano-anthracene (3b)

trans-11,12-Bis(methanesulfonylmethyl)-9,10-dihydro-9,10-ethano-anthracene was prepared in 67% yield according to the procedure described above for **3a**. ^{1}H-NMR (500.0 MHz, $CDCl_3$, δ): 7.25 (m, 4H, C_6H_4), 7.10 (m, 4H, C_6H_4), 4.28 (s, 2H, bridgehead C–*H*), 3.83 (dd, 2H, $J = 5.8$, 10.1 Hz, CH_2), 3.67 (t, 2H, $J_{HH} = 10.1$ Hz, CH_2), 2.93 (s, 6H, CH_3SO_3), 1.79 (m, 2H, ethano bridge C–*H*). $^{13}C\{^1H\}$-NMR (125.65 MHz, $CDCl_3$, δ): 142.12 (s), 141.3 (s), 126.8 (s), 126.4 (s), 125.6 (s), 123.9 (s), 67.9 (s), 37.6 (s), 37.4 (s) 30.9 (s), 25.6 (s).

2.1.7. Synthesis of cis-11,12-bis(2,3,4,5-tetramethylphospholylmethyl)-9,10-dihydro-9,10-ethano-anthracene (4a)

A solution of 1-phenyl-2,3,4,5-tetramethylphosphole (4.35 g, 20.1 mmol) in THF (40 ml) was stirred with lithium powder (0.55 g, 79.2 mmol) under an argon atmosphere for 2 h, after which the solution turned intense red. After filtering, the phenyl lithium by-product was quenched by addition of anhydrous aluminum chloride (0.89 g, 6.70 mmol) to an ice-cold solution of the reaction mixture. After stirring at 0 °C for 30 min, a solution of **3a** (3.80 g, 9.0 mmol) in THF was added dropwise. The reaction mixture was allowed to warm to r.t. and then heated at reflux overnight. After cooling to r.t., the solvent was removed under reduced pressure and the resulting gummy residue extracted into CH_2Cl_2 (100 ml), filtered, washed with degassed water (3 × 50 ml) and the organic phase separated and dried over $MgSO_4$. After filtration, the solvent was removed to give a white solid which was washed with 40:60 petroleum–ether (3 × 40 ml) and crystallized from CH_2Cl_2 at −78 °C to afford **4a** as a white solid in 68% yield (3.13 g). ^{1}H-NMR (500.0 MHz, $CDCl_3$, δ): 7.34–7.02 (m, 8H, $C_6\mathit{H}_4$), 4.52 (s, 2H, bridgehead C*H*), 2.12 (br m, 2H, ethano bridge C–*H*), 2.01 (d, 6H, *J* = 10.4 Hz, phosphole-CH_3), 1.84 (s, 6H, phosphole-CH_3), 1.82 (d, 6H, *J* = 10.4 Hz, phosphole-CH_3), 1.81 (s, 6H, phosphole-CH_3), 1.41 (m, 2H, CH_aH$_b$), 1.08 (m, 2H, CH $_a\mathit{H}_b$). ^{31}P{^{1}H}-NMR (202.0 MHz, $CDCl_3$, δ): 6.67 (s, phosphole-P). ^{13}C{^{1}H)-NMR (125.65 MHz, $CDCl_3$, δ): 144.0 (s, C_6H_4), 142.1 (d, J_{PC} = 76.0 Hz, phosphole ring), 140.9 (s, C_6H_4), 135.1 (d, J_{PC} = 108.1 Hz, phosphole ring), 126.1–123.2 (C_6H_4), 48.0 (d, J_{PC} = 10.3 Hz, bridgehead *C*–H), 39.8 (s, ethano bridge *C*–H), 25.7 (d, J_{PC} = 17.6 Hz, $\mathit{C}H_2$), 14.3 (d, J_{PC} = 21.7 Hz, $\mathit{C}H_3$), 13.2 (d, J_{PC} = 21.6 Hz, $\mathit{C}H_3$).

*2.1.8. Synthesis of trans-11,12-bis((2,3,4,5-tetramethylphospholylmethyl)-9,10-dihydro-9,10-ethano-anthracene **(4b)***

Compound **4b** was prepared from *trans*-11,12-bis-(methanesulfonylmethyl)-9,10-dihydro-9,10-ethano-anthracene in 79% yield according to the procedure described above. ^{1}H-NMR (500.0 MHz, $CDCl_3$, δ): 7.24–7.01 (m, 8H, $C_6\mathit{H}_4$), 4.16 (s, 2H, bridgehead C–*H*), 2.00 (d, 6H, *J* = 10.6 Hz, phosphole-CH_3), 1.84 (m, 6H, phosphole-CH_3), 1.82 (d, 6H, *J* = 10.6 Hz, phosphole-CH_3), 1.80 (s, 6H, phosphole-CH_3), 1.45 (dd, 2H, *J* = 14.4, 2.1 Hz, CH_aH$_b$), 1.35 (m, 2H, ethano bridge C–H), 1.42 (m, 2H, CH$_a\mathit{H}_b$), 1.28 (m, 4H, CH_2). ^{31}P{^{1}H}-NMR (202.0 MHz, $CDCl_3$, δ): 6.57 (s, phosphole-P). ^{13}C{^{1}H)-NMR (125.65 MHz, $CDCl_3$, δ): 144.5 (s, C_6H_4), 142.6 (d, J_{PC} = 33.6 Hz, phosphole ring), 140.5 (s, C_6H_4), 134.6 (d, J_{PC} = 101.8 Hz, phosphole ring), 126.2 (s, C_6H_4), 126.1 (s, C_6H_4), 125.7 (s, C_6H_4), 123.2 (s, C_6H_4), 48.8 (d, J_{PC} = 7.3 Hz, bridgehead *C*–H), 47.4 (d, J_{PC} = 10.3 Hz, ethano bridge *C*–H), 29.8 (d, J_{PC} = 19.5 Hz, $\mathit{C}H_2$), 14.3 (d, J_{PC} = 22.6 Hz, phosphole-$\mathit{C}H_3$), 13.4 (d, J_{PC} = 21.7 Hz, phosphole-CH_3).

*2.1.9. Synthesis of 1,4-bis(2,3,4,5-tetramethylphospholyl)butane **(4c)***

Compound **4c** was prepared from 1,4-dibromobutane in 45% yield according to the procedure described above. ^{1}H-NMR (500.0 MHz, $CDCl_3$, δ): 1.90 (d, 12H, *J* = 10.3 Hz, phosphole-CH_3), 1.81 (s, 12H, phosphole-CH_3), 1.58 (br m, 4H, CH_2), 1.08 (br m, 4H, CH_2). ^{31}P{^{1}H}-NMR (202.0 MHz, $CDCl_3$, δ): 12.28 (s, phosphole-P).

*2.1.10. Synthesis of cis-11,12-bis(diphenylphosphinomethyl)-9,10-dihydro-9,10-ethano-anthracene **(5a)***

A solution of diphenylphosphine (3.86 ml, 22 mmol) in THF (15 ml) was cooled to −78 °C and was treated with a 2.5 M solution of butyl lithium in hexanes (8.93 ml, 22 mmol) with rapid stirring. After warming to r.t. and stirring for an additional 30 min, the solution was cooled in an ice bath and a THF solution of *cis*-11,12-bis(methanesulfonylmethyl)-9,10-dihydro-9,10-ethano-anthracene (4.1 g, 10 mmol) added dropwise. The reaction mixture was left to warm to r.t. and stirred overnight during which time there was a gradual color change from deep orange–red to pale yellow. The solvent was removed under reduced pressure and the resulting oily residue was dissolved in Et_2O (100 ml) and washed with degassed water (30–40 ml). The organic phase was separated, dried over $MgSO_4$, filtered and the solvent removed to afford *cis*-11,12-bis-(diphenylphosphinomethyl)-9,10-dihydro-9,10-ethano-anthracene (**5a**) in 54% yield (3.2 g). ^{1}H-NMR (500.0 MHz, $CDCl_3$, δ): 6.95–7.80 (m, 28H, $C_6\mathit{H}_5$ and $C_6\mathit{H}_4$), 4.54 (s, 2H, bridgehead C–*H*), 1.95 (br s, 2H, ethano bridge C–*H*), 1.40 (m, 4H, CH_2). ^{31}P{^{1}H}-NMR (202.0 MHz, $CDCl_3$, δ): −17.9. ^{13}C{^{1}H}-NMR (125.65 MHz, $CDCl_3$, δ): 143.6–123.6 (C_6H_4 and C_6H_5), 49.9 (d, J_{PC} = 9.4 Hz), 38.4 (d, J_{PC} = 14.6 Hz), 30.1 (d, J_{PC} = 12.3 Hz).

*2.1.11. Synthesis of trans-11,12-bis(diphenylphosphinomethyl)-9,10-dihydro-9,10-ethano-anthracene **(5b)***

Compound **5b** was isolated as a white solid from the reaction between *trans*-11,12-bis(methanesulfonylmethyl)-9,10-dihydro-9,10-ethano-anthracene and lithium diphenylphosphide according to the procedure described above for **5a**. ^{1}H NMR (500.0 MHz, $CDCl_3$, δ): 6.9–7.60 (m, 28H, $C_6\mathit{H}_4$ and $C_6\mathit{H}_5$), 4.26 (s, 2H, bridgehead C–*H*), 1.80 (m, 2H, ethano bridge C–*H*), 1.52 (m, 4H, CH_2). ^{13}C{^{1}H}-NMR (125.65 MHz, $CDCl_3$, δ): 143.8–123.3 (C_6H_5 and C_6H_4), 48.9 (d, J_{PC} = 13.4 Hz), 45.6 (dd, J_{PC} = 19.7 Hz), 34.6 (dd, J_{PC} = 10.3 Hz).

*2.1.12. Synthesis of [{cis-11,12-bis-(2,3,4,5-tetramethylphospholylmethyl)-9,10-dihydro-9,10-ethano-anthracene}PdCl$_2$] **(6a)***

A solution of [(cycloocta-1,5-diene)$PdCl_2$] (0.27 g, 0.95 mmol) in CH_2Cl_2 was treated with a CH_2Cl_2 solution of 11,12-bis-(2,3,4,5-tetramethylphospholylmethyl)-9,10-dihydro-9,10-ethano-anthracene (0.48 g, 0.95 mmol) and stirred vigorously for ca. 30 min. The reaction mixture was filtered, the solvent removed under vacuum and the resulting yellow solid washed with *n*-hexane (~ 20 ml) and dried under vacuum to give **6a** as a pale yellow solid in 73% yield (0.48 g). Crystallization from a concentrated CH_2Cl_2 solution layered with *n*-hexane gave X-ray quality crystals of **6a**. ^{1}H-NMR (500.0 MHz, $CDCl_3$, δ): 7.2 (dd, 2H, *J* = 5.5, 3.0 Hz, $C_6\mathit{H}_4$), 7.15 (dd, 2H, *J* = 5.5, 3.7 Hz, $C_6\mathit{H}_4$), 7.10 (dd, 2H, *J* = 5.2, 3.1 Hz, $C_6\mathit{H}_4$), 7.07 (dd, 2H, *J* = 5.2, 3.1 Hz, $C_6\mathit{H}_4$), 3.93 (s, 2H, bridgehead C–*H*), 2.49 (m, 2H, ethano bridge C–*H*), 2.08 (d, 6H, *J* = 11.9 Hz, phosphole-CH_3), 1.89 (s, 6H, phosphole-CH_3), 1.87 (d, 6H, $J = 11.9$ Hz, phosphole-CH_3), 1.84 (s, 6H, phosphole-CH_3), 1.38 (m, 4H, CH_2). ^{31}P{^{1}H}-NMR (202.0 MHz, CDCl$_3$, δ): 42.3 (s, phosphole-P). Anal. Calc. for $C_{34}H_{40}Cl_2P_2Pd$: C, 59.38; H, 5.86. Found: C, 59.63; H, 5.79%.

Compounds **6b–d** were prepared according to the procedure described above.

2.1.13. Synthesis of [{trans-11,12-bis-(2,3,4,5-tetramethylphospholylmethyl)-9,10-dihydro-9,10-ethano-anthracene}PdCl$_2$] (*6b*)

Compound **6b** was isolated as pale yellow X-ray quality crystals in 68% yield by slow diffusion of *n*-hexane into a concentrated CHCl$_3$ solution at r.t. ^{1}H-NMR (500.0 MHz, CDCl$_3$, δ): 7.13 (dd, 2H, $J = 7.7$, 1.6 Hz, C$_6H_4$), 7.10 (dd, 2H, $J = 7.0$, 1.2 Hz, C$_6H_4$), 7.07 (dd, 2H, $J = 7.7$, 1.6 Hz, C$_6H_4$), 7.13 (dd, 2H, $J = 7.0$, 1.2 Hz, C$_6H_4$), 3.86 (s, 2H, bridgehead C–H), 2.07 (d, 6H, $J = 11.9$ Hz, phosphole-CH_3), 1.87 (s, 6H, phosphole-CH_3), 1.86 (d, 6H, $J = 11.9$ Hz, phosphole-CH_3), 1.80 (s, 6H, phosphole-CH_3), 1.74 (m, overlapping 2H, CH_aH$_b$, 2H, ethano bridge C-H), 1.54 (m, 2H, CH$_a$$H_b$). ^{31}P{^{1}H}-NMR (202.0 MHz, CDCl$_3$, δ): 41.8 (s, phosphole-P). ^{13}C{^{1}H)-NMR (125.65 MHz, CDCl$_3$, δ): 143.4 (s, C_6H$_4$), 138.1 (s, C_6H$_4$), 132.1 (d, $J_{PC} = 67.0$ Hz, phosphole ring), 130.2 (d, $J_{PC} = 51.2$ Hz, phosphole ring), 126.9 (s, C_6H$_4$), 126.4 (s, C_6H$_4$), 125.6 (s, C_6H$_4$), 123.1 (s, C_6H$_4$), 51.8 (s, bridgehead C–H), 45.7 (s, ethano bridge C–H), 38.5 (d, $J_{PC} = 23.6$ Hz, CH$_2$), 14.2 (d, $J_{PC} = 19.5$ Hz, phosphole-CH$_3$), 13.8 (d, $J_{PC} = 26.2$ Hz, phosphole-CH$_3$). Anal. Calc. for $C_{34}H_{40}Cl_2P_2Pd\cdot 3CHCl_3$: C, 42.47; H, 4.14. Found: C, 42.83; H, 3.94%.

2.1.14. Synthesis of [{cis-11,12-bis(diphenylphosphinomethyl)-9,10-dihydro-9,10-ethano-anthracene}-PdCl$_2$] (*6c*)

Compound **6c** was isolated as pale yellow crystals in 74% yield by slow diffusion of Et$_2$O into a concentrated CH$_2$Cl$_2$ solution. X-ray quality crystals can be grown by slow diffusion of *n*-hexane into a concentrated CHCl$_3$ solution at r.t. ^{1}H-NMR (500.0 MHz, CDCl$_3$, δ): 7.18–7.50 (m, 28H, C$_6H_5$ and C$_6H_4$), 3.60 (s, 2H, bridgehead C–H), 1.88 (m, 2H, ethano bridge C–H), 1.18 (br s, 4H, CH_2). ^{31}P{^{1}H}-NMR (202.0 MHz, CDCl$_3$, δ): 32.3. Anal. Calc. for $C_{42}H_{36}Cl_2P_2Pd$: C, 64.70; H, 4.65. Found: C, 64.29; H, 4.88%.

2.1.15. Synthesis of [{trans-11,12-bis(diphenylphosphinomethyl)-9,10-dihydro-9,10-ethano-anthracene}-PdCl$_2$] (*6d*)

Compound **6d** was isolated as pale yellow X-ray quality crystals in 68% yield by slow diffusion of *n*-hexane into a concentrated CH$_2$Cl$_2$ solution at r.t. ^{1}H-NMR (500.0 MHz, CDCl$_3$, δ): 7.70 (dd, 4H, $J_{HH} = 8.0$, 11.6 Hz, C$_6H_4$/C$_6H_5$), 7.50 (t, 2H, $J_{HH} = 7.6$ Hz, C$_6H_4$/C$_6H_5$), 7.30 (m, 8H, C$_6H_4$/C$_6H_5$), 7.25 (dt, 4H, $J_{HH} = 2.7$, 7.9 Hz, C$_6H_4$/C$_6H_5$), 7.05 (m, 8H, C$_6H_4$/C$_6H_5$), 6.90 (d, 2H, $J_{HH} = 6.7$ Hz, C$_6H_4$/C$_6H_5$), 3.36 (s, 2H, bridgehead C–H), 2.35 (dt, 2H, $J_{HH} = 4.3$, 5.6 Hz, ethano bridge C–H). ^{31}P{^{1}H}-NMR (202.0 MHz, CDCl$_3$, δ): 29.7. Anal. Calc. for $C_{43}H_{38}Cl_4P_2Pd$: C, 59.72; H, 4.42. Found: C, 59.80; H, 4.77%.

2.1.16. Synthesis of [{1,4-bis(2,3,4,5-tetramethylphospholyl)butane}PdMeCl] (*6e*)

A solution of [(cycloocta-1,5-diene)PdMeCl] (0.250 g, 1.0 mmol) in CH$_2$Cl$_2$ (10 ml) was treated with a CH$_2$Cl$_2$ solution (7–10 ml) of 1,4-bis(2,3,4,5-tetramethylphospholyl)butane (0.334 g, 1.0 mmol) and stirred vigorously for ca. 3–4 h. The reaction mixture was filtered, the residue washed with hexane (2 × 10 ml) to give **6e** as a pale yellow powder in 68% yield (0.39 g). ^{1}H-NMR (200.1 MHz, CDCl$_3$, δ): 1.91 (br s, 4H, CH_2), 1.84 (br s, 12H, phosphole-CH_3), 1.80 (br, 16H, phosphole-CH_3 + CH_2), 1.08 (br, 3H, Pd–CH_3). ^{31}P{^{1}H}-NMR (202.0 MHz, CDCl$_3$, δ): 41.7 (s).

2.1.17. Synthesis of [{cis-11,12-bis(2,3,4,5-tetramethylphospholylmethyl)-9,10-dihydro-9,10-ethano-anthracene}Pd(OAc)$_2$] (*7a*)

A suspension of palladium acetate (0.23 g, 1.06 mmol) in toluene (~1–2 ml) was treated with a toluene solution (~5–7 ml) of *cis*-11,12-bis-(2,3,4,5-tetramethylphospholylmethyl)-9,10-dihydro-9,10-ethano-anthracene (0.54 g, 1.06 mmol) and stirred vigorously for ca. 30 min during which time a pale solid precipitated from solution. The reaction mixture was filtered and the precipitate was washed with toluene (2 × 3 ml) and hexane (3 × 10 ml), and dried under vacuum to give **7a** as a yellow powder in 48% yield (0.36 g). ^{1}H-NMR (500.0 MHz, CDCl$_3$, δ): 7.07–7.21 (m, 8H, C$_6H_4$), 3.93 (s, 2H, bridgehead C–H), 2.57 (m, 2H, ethano bridge C–H), 2.15 (d, 6H, $J = 11.3$ Hz, phosphole-CH_3), 1.84 (m, 18H, phosphole-CH_3), 1.80 (br s, 6H, CH_3CO$_2$), 1.43 (m, 4H, CH_2). ^{31}P{^{1}H}-NMR (202.0 MHz, CDCl$_3$, δ): 44.5 (s, phosphole-P).

Catalyst precursors **7c** and **d** were prepared using a procedure similar to that described for **7a**.

2.1.18. Synthesis of [{cis-11,12-bis(diphenylphosphinomethyl)-9,10-dihydro-9,10-ethano-anthracene}-Pd(OAc)$_2$] (*7c*)

Compound **7c** was isolated as a yellow powder in 69% yield. ^{1}H-NMR (500.0 MHz, CDCl$_3$, δ): 7.20–7.58 (m, 28H, C$_6H_5$ and C$_6H_4$), 3.86 (s, 2H, bridgehead C–H), 2.28 (m, 2H, ethano bridge C–H), 1.42–1.70 (m, 6H, CH_3), 0.70 (m, 4H, CH_2). ^{31}P{^{1}H}-NMR (202.0 MHz, CDCl$_3$, δ): 24.1.

*2.1.19. Synthesis of [{trans-11,12-bis(diphenylphosphinomethyl)-9,10-dihydro-9,10-ethanoanthracene}Pd(OAc)$_2$] (**7d**)*

Compound **7d** was isolated as a yellow powder in 62% yield. ^{1}H-NMR (500.0 MHz, CDCl$_3$, δ): 6.50–7.95 (m, 28H, C_6H_4 and C_6H_5), 3.73 (br s, 2H, bridgehead C–H), 2.28 (s, 2H, ethano bridge C–H), 1.85 (m, 6H, CH_3), 1.48 (s, 4H, CH_2). ^{31}P{^{1}H}-NMR (202.0 MHz, CDCl$_3$, δ): 23.1. ^{13}C{^{1}H}-NMR (125.65 MHz, CDCl$_3$, δ): 144–123 (C_6H$_4$ and C_6H$_5$), 50.9 (bridgehead C–H), 44.1 (ethano bridge C–H), 36.6 (d, $J_{PC} = 14.1$ Hz, CH$_2$).

2.2. Polymerization procedure

Polymerizations were conducted in MeOH in a 300 ml Parr bench-mounted reactor. The catalyst precursors [(P–P)Pd(OAc)$_2$] were prepared according to the procedure described above. In a typical procedure, 0.085 mmol of [(P–P)Pd(OAc)$_2$] was dissolved in 60 ml of anhydrous MeOH, 0.85 mmol of CH_3SO_3H added and the solution transferred to a 300 ml autoclave under N_2. Alternatively, the catalyst can be generated prior to charging the reactor by stirring a CH_2Cl_2 solution of diphosphine (0.085 mmol) and palladium acetate (0.085 mmol) for ca. 15 min before removing the solvent under reduced pressure and redissolving the residue in MeOH before adding CH_3SO_3H. The reaction mixture was pressurized to 20 bar with an equimolar mixture of CO and ethylene and heated at 90 °C for 2 h. The reaction was quenched by release of CO–ethylene pressure and the polymer was isolated by filtration, dried and weighed and the filtered solution analyzed by gas chromatography. Provided the catalyst mixtures are generated with the exclusion of oxygen using Schlenk techniques, the same results could be obtained with catalyst prepared by both methods, i.e. using complexes either prepared in advance or generated in CH_2Cl_2, prior to polymerization.

*2.3. Crystal structure determination of **6a–d***

All measurements were made on a Bruker AXS SMART 1K CCD area-detector diffractometer using graphite-monochromated Mo–K$_\alpha$ radiation ($\lambda = 0.71073$ Å) and narrow frame exposures (0.3° in ω). Cell parameters were refined from all strong reflections in each data set. Intensities were corrected semi-empirically for absorption, based on symmetry-equivalent and repeated reflections. No significant intensity decay was

Table 1

Crystal data and structure refinement parameters for compounds **6a**–**d**

Compound	**6a**·2CH$_2$Cl$_2$	**6b**·3CHCl$_3$	**6c**·2CHCl$_3$	**6d**·CH$_2$Cl$_2$
Empirical formula	$C_{36}H_{44}Cl_6P_2Pd$	$C_{37}H_{43}Cl_{11}P_2Pd$	$C_{44}H_{38}Cl_8P_2Pd$	$C_{43}H_{38}Cl_4P_2Pd$
Formula weight	857.75	1046.00	1018.68	864.87
Temperature (K)	160	160	160	160
Crystal system	Triclinic	Monoclinic	Monoclinic	Monoclinic
Space group	$P\bar{1}$	$P2_1/n$	$P2_1/c$	$P2_1/c$
Unit cell dimensions				
a (Å)	11.1072(6)	11.2206(4)	12.6042(6)	14.4531(10)
b (Å)	12.1233(7)	17.9819(6)	19.7955(9)	16.2930(12)
c (Å)	16.9939(10)	22.2659(7)	17.6945(8)	16.8625(12)
α (°)	69.628(2)			
β (°)	87.862(2)	93.742(1)	105.300(2)	104.921(1)
γ (°)	67.256(2)			
V (Å^3)	1965.83(19)	4483.0(3)	4258.4(3)	3837.0(5)
Z	2	4	4	4
Absorption coefficient (mm^{-1})	0.986	1.168	1.046	0.877
Crystal size (mm)	0.50 × 0.40 × 0.40	0.60 × 0.50 × 0.50	0.40 × 0.30 × 0.20	0.75 × 0.65 × 0.55
θ_{max} (°)	28.5	28.4	28.6	28.5
Reflections measured	16194	37645	36140	26221
Unique reflections	8560	10547	10081	8943
Reflections with $F^2 > 2\sigma(F^2)$	7752	9397	6856	7589
R_{int} (on F^2)	0.0271	0.0231	0.0615	0.0332
No. of parameters	414	468	496	463
R [a] [$F^2 > 2\sigma(F^2)$]	0.0667	0.0674	0.0854	0.0536
R_w [b] (all data)	0.1452	0.1655	0.2504	0.1313
Goodness-of-fit [c] (S)	1.304	1.061	1.108	1.059
Largest difference peak and hole (e Å^{-3})	1.99 and −1.61	2.18 and −2.18	2.06 and −1.82	2.86 and −3.34

[a] Conventional $R = \Sigma||F_o| - |F_c||/\Sigma|F_o|$ for 'observed' reflections having $F_o^2 > 2\sigma(F_o^2)$.

[b] $[\Sigma(wF_o^2 - F_c^2)^2/\Sigma w(F_o^2)^2]^{1/2}$ for all data.

[c] Goodness-of-fit $= [\Sigma w(F_o^2 - F_c^2)^2/(\text{no. of unique reflections} - \text{no. of parameters})]^{1/2}$.

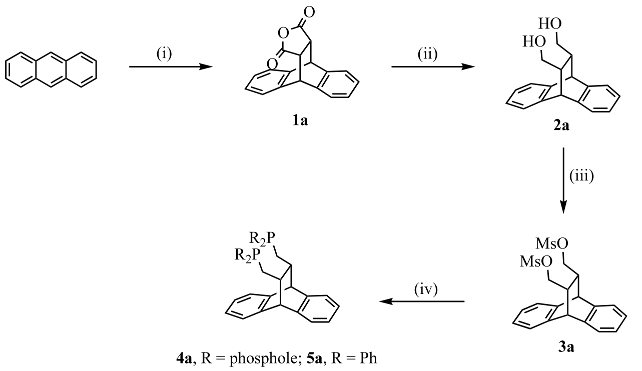

Scheme 1. (i) One equivalent $AlCl_3$, maleic anhydride; (ii) $LiAlH_4$, ether; (iii) MsCl, pyridine; (iv) $LiPPh_2$ or (2,3,4,5-tetramethyl phospholyl)lithium in THF.

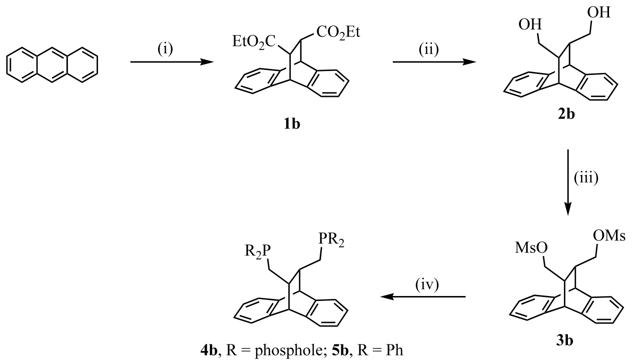

Scheme 2. (i) One equivalent $AlCl_3$, diethylfumarate; (ii) $LiAlH_4$, ether; (iii) MsCl, pyridine; (iv) $LiPPh_2$ or (2,3,4,5-tetramethyl phospholyl)lithium in THF.

observed. The structures were solved by direct methods (Patterson synthesis for **6d**) and refined on F^2 values for all unique data by full-matrix least-squares. Table 1 gives further details. All non-hydrogen atoms were refined anisotropically. Hydrogen atoms located in difference maps were constrained with a riding model; U(H) was set at 1.2 (1.5 for methyl groups) times U_{eq} for the parent atom. The solvent molecule in **6d** is disordered. The largest residual peaks are close to Pd and Cl atoms; these and relatively high displacement parameters for solvent molecules may indicate further unresolved disorder. Programs used were SHELXTL [16] for structure solution, refinement and molecular graphics, Bruker AXS SMART (control) and SAINT (integration) and local programs [17].

3. Results and discussion

3.1. Synthesis and coordination chemistry of anthracene-bridged diphosphines and phospholes *4a* and *b* and *5a* and *b*

Ligands **4a** and **b** and **5a** and **b** were prepared according to the procedure outlined in Schemes 1 and 2, by reacting the corresponding dimesylate with 2,3,4,5-tetramethylphospholyl lithium and lithium diphenyl phosphide, respectively. The anhydride 9,10-dihydrido-9,10-ethano-anthracene-11,12-dicarboxylic acid-anhydride (**1a**) and diester *trans*-9,10-dihydrido-9,10-ethano anthracene-dicarboxylic acid-(11,12)-diethyl ester (**1b**) were isolated in near quantitative yields from the Diels–Alder cycloaddition of anthracene with maleic anhydride and diethyl fumarate, respectively, in the presence of a stoichiometric amount of aluminum trichloride. Reduction of the anhydride and diester with lithium aluminum hydride gave the corresponding diol **2**, which was converted into its mesylate **3** by reaction with methane sulfonyl choride in pyridine. The mesylate was chosen since all attempts to convert the diol into the corresponding bromomethyl derivative resulted in the formation of intractable solids. Dropwise addition of a THF solution of lithium 2,3,4,5-tetramethyl phospholyl or diphenylphosphide into a THF solution of the mesylate gave **4a** and **b** and **5a** and **b**, respectively, as evidenced by the disappearance of the intense color associated with the lithium salt.

The $^{31}P\{^1H\}$-NMR spectra of **4a** and **b** and **5a** and **b** each contain a single resonance in the region expected for a uncoordinated phosphine or phosphole. The ^1H-NMR spectrum of **4a** contains four signals associated with the methyl groups attached to the phosphole rings, two doublets at δ 2.01 ($J_{PH} = 10.4$ Hz) and 1.82 ($J_{PH} = 10.4$ Hz) and two singlets at δ 1.84 and 1.81, as well as a singlet at δ 4.53 belonging to the protons attached to the central six-membered ring, a complex multiplet at δ 1.41 for the diastereotopic methylene protons, and a multiplet at δ 1.08 corresponding to the protons attached to the ethane bridge. The ^1H-NMR spectrum of **4b** shows a similar set of resonances and is consistent with the expected formulation. A full spectroscopic assignment of **4a** and **b** has been undertaken using ^1H–^1H COSY, $^1H\{^{31}P\}$ and ^1H–^{13}C heteronuclear single- and multiple-bond correlation studies.

The bis(phosphole), 1,4-bis(2,3,4,5-tetramethylphospholyl)butane (**4c**) [18] has also been prepared in order to undertake comparative catalyst testing with systems based on the more common C_4-bridged diphosphine 1,4-bis(diphenylphosphino)butane (dppb), to definitively assess the influence of the phospholyl ring on catalyst activity and selectivity. Phosphole **4c** was prepared by addition of a tetrahydrofuran solution of lithium 2,3,4,5-tetramethylphospholyl into a solution of 1,4-dibromobutane according to previously published procedures (Eq. (2)). The ^1H- and $^{13}C\{^1H\}$-NMR spectra are consistent with the expected formulation, the former containing a doublet at δ 1.90 ($J_{PH} = 10.3$ Hz) and a singlet at δ 1.81, belonging to the 2,5- and 3,4-methyl groups attached to the phosphole ring, respectively, and two broad high-field multiplets associated with the methylene groups of the butane tether.

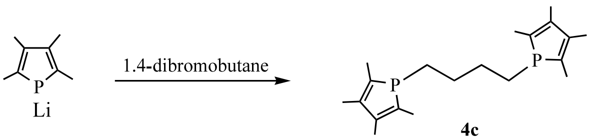

4c (2)

Addition of a dichloromethane solution of **4a** and **b** and **5a** and **b** into a dichloromethane solution of [{cycloocta-1,5-diene}PdCl$_2$] resulted in a gradual color change from yellow to orange with the formation of [(P–P)PdCl$_2$] (P–P = **4a**, **6a**; P–P = **4b**, **6b**; P–P = **5a**, **6c**; P–P = **5b**, **6d**), in yields of up to 70% (Eqs. (3) and (4)). The $^{31}P\{^1H\}$-NMR spectra of **6a**–**d** each contain sharp singlets characteristic of a coordinated diphosphine. In the ^1H-NMR spectrum of **6a**, four signals are found, two doublets at δ 2.08 and 1.87 ($J_{PH} = 11.9$ Hz) and two singlets at δ 1.89 and 1.84, which belong to the 2,5- and 3,4-methyl groups of the phosphole ring, respectively. The magnitude of J_{PH} is similar to that in 1-phenyl 2,3,4,5-tetramethylphosphole and its palladium complex [19]. Complex multiplets centered at δ 1.38 and 2.49 are consistent with diastereotopic methylene protons and the protons attached to the ethano bridge, respectively, and a singlet at δ 3.93 belongs to the bridgehead protons, i.e. those attached to the central six-membered ring. In addition, the aromatic protons appear as a characteristic set of four well-separated doublets of doublets at δ 7.20, 7.15, 7.10 and 7.07.

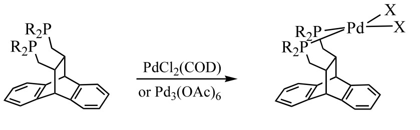

(3)

6a, R = phosphole; **6c**; R = Ph; X = Cl
7a, R = phosphole; **7c**, R = Ph; X = OAc

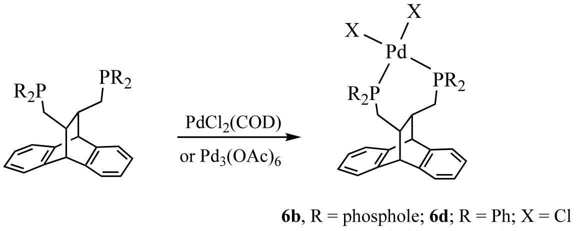

(4)

6b, R = phosphole; **6d**; R = Ph; X = Cl
7b, R = phosphole; **7d**, R = Ph; X = OAc

Unexpectedly, addition of a dichloromethane solution of 1,4-bis(2,3,4,5-tetramethylphospholyl)butane to a solution of [{cycloocta-1,5-diene}PdCl$_2$] resulted in the immediate formation of a red precipitate which was too insoluble to characterize using conventional spectroscopic techniques. Reaction of 1,4-bis(2,3,4,5-tetramethylphospholyl)butane with [{cycloocta-1,5-diene}PdMeCl] in dichloromethane resulted in the formation of a colorless solution from which an off-white solid was isolated by precipitation. Unexpectedly, the room temperature $^{31}P\{^1H\}$-NMR spectrum of this product contains a single sharp resonance at δ 41.7 and not the two signals that would be predicted for inequivalent phosphole groups *trans* to methyl and chloride. The presence of a single ^{31}P resonance is consistent with a *trans* arrangement of methyl and chloride, indicating that [{1,4-bis(2,3,4,5-tetramethylphospholyl)butane}-PdMeCl] most likely exists as a polymer/oligomer (Eq. (5)). The alternative explanation that **4c** coordinates in a bidentate manner and that the two phosphole groups are rendered equivalent by a rapid fluxional process has been eliminated by undertaking a variable temperature $^{31}P\{^1H\}$-NMR study which showed no evidence of line broadening.

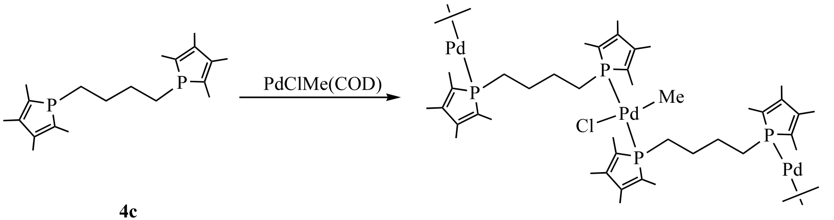

4c **6e** (5)

The catalyst precursors [(P–P)Pd(OAc)$_2$] (**7a**, **7c** and **d**) were prepared by the addition of a concentrated solution of the corresponding diphosphine to a rapidly stirred suspension of [Pd$_3$(OAc)$_6$] [20] to give a light colored precipitate which was filtered, washed with toluene and hexane and dried to afford the desired compounds as spectroscopically pure solids. Attempts to prepare **7b** resulted in the formation of a mixture of compounds; therefore, the catalyst precursor was generated *in situ* prior to catalyst testing. The $^{31}P\{^1H\}$- and ^1H-NMR spectroscopic characteristics of these compounds bear a close similarity to those of their dichloride counterparts.

3.2. X-ray crystal structures of anthracene-bridged diphosphine and phosphole complexes *6a–d*

The lack of structural data for palladium(II) complexes of bidentate phospholes prompted us to undertake single-crystal X-ray analyses of **6a** and **b**. Single crystals of **6a**·2CH$_2$Cl$_2$ and **6b**·3CHCl$_3$ suitable for X-ray analysis were grown from a dichloromethane solution layered with hexane and a chloroform solution layered with hexane, respectively. Perspective views of the molecular structures of **6a** and **b** together with the atomic numbering scheme are illustrated in Figs. 1 and 2, respectively, and a selection of relevant bond lengths and angles is listed in Table 2 while crystal data are provided in Table 1. Since the structures of both compounds are based on bidentate phospholes bridged by a C_4-ethano anthracene tether and are clearly related, they will be described together. In both **6a** and **b**, the coordination sphere around palladium is close to square planar, as indicated by the dihedral angle of 2.9° (**6a**) and 8.5° (**6b**) between the planes containing P(1)Pd(1)P(2) and Cl(1)Pd(1)Cl(2), and **4a** and **b** both form seven-membered chelate rings. The Pd–P bond lengths in **6a** [Pd(1)–P(1) = 2.2392(14) Å, Pd(1)–P(2) = 2.2455(14) Å] are similar to those in **6b** [Pd(1)–P(1) = 2.2498(11) Å, Pd(1)–P(2) = 2.2506(11) Å], slightly longer than those in the phosphole complex [{1,2-bis(2,3,4,5-tetramethylphospholylmethyl)benzene}-$PdCl_2$] [12] but within the range expected for palladium complexes of diphosphines, including [Pd(BIPHOS)Cl_2] [21] and [Pd(DMPP)$_2$$Cl_2$] [22]. The distances and angles in the phosphole rings are similar to those previously reported for related compounds, including [Pd-(bidmpp)$_2$][BF_4]$_2$ [23], [Pd(BIPHOS)Cl_2] [21], *trans*-[Pd(DMPP)$_2$$X_2$] [24], [Pd(TMBA)(DMPP)Cl] [25] and [Pd(TMBA)(DMPP)(NO_3)] [26] and are consistent with localized double and single bonds. The two phosphole rings in **6a** are essentially planar and approximately parallel forming a dihedral angle of 20.2° and oriented perpendicular to the PdP_2Cl_2 plane. In contrast, the dihedral angle between the phosphole rings in **6b** is considerably greater (33.6°) presumably reflecting the torsional twist enforced by the *trans* geometry at the ethane carbon–carbon bond bridging the anthracene fragment. The natural bite angles of 100.30 (1) and 98.62(5)°, for **6a** and **6b**, respectively, are greater than that in [$PdCl_2$(dppb)] [27] and much closer to the value reported in the palladium dichloride complex of the C_4-tethered diphosphine 2,2-dimethyl-4,5-bis(diphenylphosphinomethyl)-1,3-dioxolane (∠PPdP = 96.78°) [28]. In both **6a** and **b**, the Cl(1)Pd(1)Cl(2) angles are close to 90° [Cl(1)–Pd(1)–Cl(2) = 91.63(5)°, **6a**;

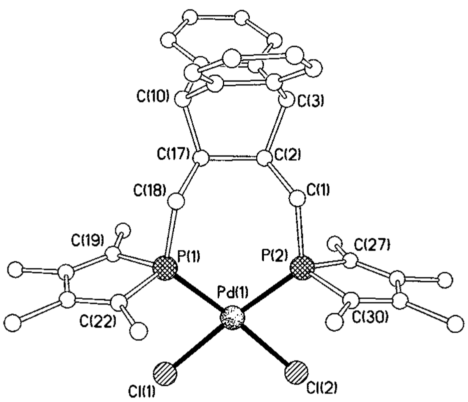

Fig. 1. Molecular structure of [{*cis*-11,12-bis(2,3,4,5-tetramethylphospholylmethyl)-9,10-dihydro-9,10-ethano-anthracene}$PdCl_2$] (**6a**). Hydrogen atoms and the CH_2Cl_2 molecules of crystallization have been omitted.

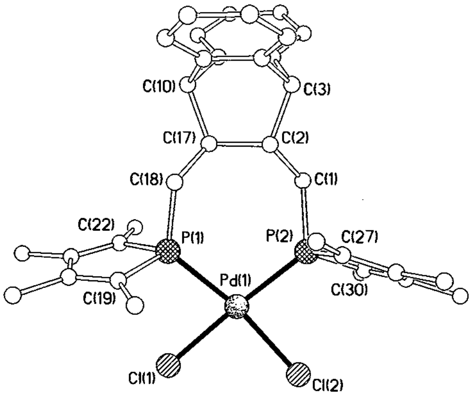

Fig. 2. Molecular structure of [{*trans*-11,12-bis(2,3,4,5-tetramethylphospholylmethyl)-9,10-dihydro-9,10-ethano-anthracene}$PdCl_2$] (**6b**). Hydrogen atoms and the $CHCl_3$ molecules of crystallization have been omitted.

Table 2
Selected bond distances (Å) and bond angles (°) for **6a** and **b**

6a		**6b**	
Bond lengths			
Pd(1)–Cl(1)	2.3553(13)	Pd(1)–Cl(1)	2.3500(13)
Pd(1)–Cl(2)	2.3662(14)	Pd(1)–Cl(2)	2.3400(12)
Pd(1)–P(1)	2.2392(14)	Pd(1)–P(1)	2.2498(11)
Pd(1)–P(2)	2.2455(14)	Pd(1)–P(2)	2.2506(11)
P(1)–C(19)	1.809(6)	P(1)–C(19)	1.799(5)
P(1)–C(22)	1.803(5)	P(1)–C(22)	1.797(5)
C(19)–C(20)	1.348(8)	C(19)–C(20)	1.334(7)
C(20)–C(21)	1.490(8)	C(20)–C(21)	1.476(7)
C(21)–C(22)	1.341(8)	C(21)–C(22)	1.350(7)
P(2)–C(27)	1.810(6)	P(2)–C(27)	1.776(5)
P(2)–C(30)	1.799(6)	P(2)–C(30)	1.800(5)
C(27)–C(28)	1.345(8)	C(27)–C(28)	1.363(7)
C(28)–C(29)	1.485(10)	C(28)–C(29)	1.479(8)
C(29)–C(30)	1.352(9)	C(29)–C(30)	1.329(7)
Bond angles			
P(1)–Pd(1)–P(2)	98.62(5)	P(1)–Pd(1)–P(2)	100.30(4)
Cl(1)–Pd(1)–Cl(2)	91.63(5)	Cl(1)–Pd(1)–Cl(2)	89.63(5)
P(1)–Pd(1)–Cl(1)	84.66(5)	P(1)–Pd(1)–Cl(1)	83.28(4)
P(2)–Pd(1)–Cl(2)	80.05(5)	P(2)–Pd(1)–Cl(2)	87.11(4)
Pd(1)–P(2)–C(30)	114.9(2)	Pd(1)–P(2)–C(30)	114.94(17)
Pd(1)–P(2)–C(1)	124.34(18)	Pd(1)–P(2)–C(1)	121.84(16)
Pd(1)–P(2)–C(27)	114.2(2)	Pd(1)–P(2)–C(27)	115.68(18)
C(30)–P(2)–C(1)	99.9(3)	C(30)–P(2)–C(1)	99.7(2)
C(1)–P(2)–C(27)	104.4(3)	C(1)–P(2)–C(27)	106.3(2)
Pd(1)–P(1)–C(18)	122.36(18)	Pd(1)–P(1)–C(18)	124.78(15)
Pd(1)–P(1)–C(19)	116.55(19)	Pd(1)–P(1)–C(19)	112.92(16)
Pd(1)–P(1)–C(22)	115.00(18)	Pd(1)–P(1)–C(22)	117.14(16)
C(18)–P(1)–C(22)	100.4(2)	C(18)–P(1)–C(22)	104.3(2)
C(18)–P(1)–C(19)	104.0(3)	C(18)–P(1)–C(19)	98.4(2)
C(19)–P(1)–C(22)	93.8(3)	C(19)–P(1)–C(22)	93.5(2)

Cl(1)–Pd(1)–Cl(2) = 89.63(5)°, **6b**] and the large natural bite angle manifests itself in compression of the two P(1)–Pd(1)–Cl(1) and P(2)–Pd(1)–Cl(2) angles which are smaller than 90° [P(1)–Pd(1)–Cl(1) = 84.66(5)°, P(2)–Pd(1)–Cl(2) = 85.05(5)°, **6a**; P(2)–Pd(1)–Cl(2) = 87.11(4)°, P(1)–Pd(1)–Cl(1) 83.28(4)°, **6b**]. Structural data suggest that bidentate phospholes behave in much the same manner as a conventional diphosphine, as σ-donor π-acceptors.

Single-crystal X-ray analyses of **6c** and **d** have also been undertaken in order to compare with related complexes of C$_4$-bridged diphosphines including *endo*, *endo* and *exo*, *endo*-[{2,3-bis(diphenylphosphinomethyl)norbornane}PdCl$_2$]. The molecular structures of **6c** and **6d** are shown in Figs. 3 and 4, respectively, and a selection of relevant bond lengths and angles is listed in Table 3 while crystal data are provided in Table 1. Both complexes have the expected square planar coordination around palladium, the dihedral angle between PdP$_2$ and PdCl$_2$ planes being 8.5 and 9.4°, for **6c** and **6d**, respectively. The structures clearly show that diphosphines **5a** and **b** bind in a chelating manner to form seven-membered rings. While the Pd–P bond lengths in **6c** are essentially equivalent [Pd(1)–P(1) = 2.2527(18) Å; Pd(1)–P(2) = 2.2543(19) Å], and in the range expected for complexes of diphosphines, there is a marked difference between the Pd–P bond lengths in **6d** [Pd(1)–P(1) = 2.2621(10) Å, Pd(1)–P(2) = 2.2911(10) Å); Δ(Pd–P) = 0.0290 Å], indicating that the interaction of one of the diphenylphosphino groups to the palladium center is significantly weaker than the other. This difference is substantially greater than the corresponding difference in **6b**, for which Δ(Pd–P) = 0.0008 Å. While the Cl–Pd–P angles in **6c** show a significant compression from 90° and are similar [Cl(1)–Pd(1)–P(1) = 84.79(7)°, Cl(2)–Pd(1)–P(2) = 85.82(7)°], there is a significant difference between the corresponding angles in **6d** [P(1)–Pd(1)–Cl(1) = 81.23(4)°, P(2)–Pd(1)–Cl(2) = 89.04°, $\Delta\angle$(PPdCl) = 7.81°]. A similar distortion is clearly evident in the structure of **6b**, although the difference $\Delta\angle$(PPdCl) = 3.83° is not as pronounced as that in **6d**. The natural bite angles P(1)PdP(2) of 99.78(7) and 100.25(3)° for **6c** and **6d**, respectively, are in the range

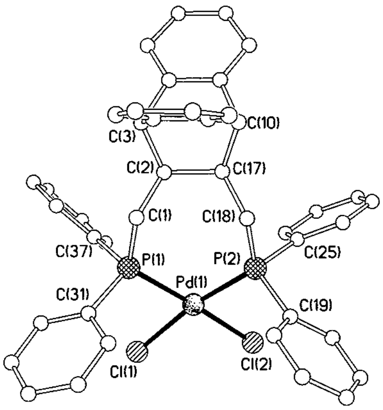

Fig. 3. Molecular structure of [{*cis*-11,12-bis(diphenylphosphinomethyl)-9,10-dihydro-9,10-ethano-anthracene}PdCl$_2$] (**6c**). Hydrogen atoms and the CHCl$_3$ molecules of crystallization have been omitted.

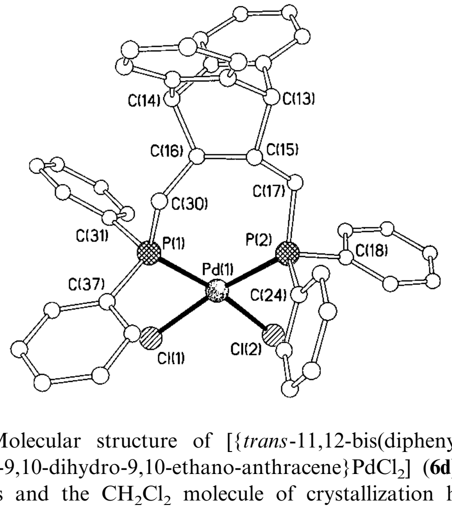

Fig. 4. Molecular structure of [{*trans*-11,12-bis(diphenylphosphinomethyl)-9,10-dihydro-9,10-ethano-anthracene}PdCl$_2$] (**6d**). Hydrogen atoms and the CH$_2$Cl$_2$ molecule of crystallization have been omitted.

Table 3
Selected bond distances (Å) and bond angles (°) for **6c** and **d**

6c		**6d**	
Bond lengths			
Pd(1)–Cl(1)	2.3472(19)	Pd(1)–Cl(1)	2.3420(10)
Pd(1)–Cl(2)	2.3618(18)	Pd(1)–Cl(2)	2.3533(9)
Pd(1)–P(1)	2.2527(18)	Pd(1)–P(1)	2.2621(10)
Pd(1)–P(2)	2.2543(19)	Pd(1)–P(2)	2.2911(10)
P(1)–C(1)	1.835(7)	P(1)–C(30)	1.828(4)
P(2)–C(18)	1.835(7)	P(2)–C(17)	1.848(4)
C(1)–C(2)	1.538(9)	C(17)–C(15)	1.518(5)
C(2)–C(17)	1.569(10)	C(15)–C(16)	1.551(5)
C(17)–C(18)	1.533(10)	C(16)–C(30)	1.540(5)
Bond angles			
P(1)–Pd(1)–P(2)	99.78(7)	P(1)–Pd(1)–P(2)	100.25(3)
Cl(1)–Pd(1)–Cl(2)	90.04(7)	Cl(1)–Pd(1)–Cl(2)	89.41(4)
P(1)–Pd(1)–Cl(1)	84.79(7)	P(1)–Pd(1)–Cl(1)	81.23(4)
P(2)–Pd(1)–Cl(2)	85.82(7)	P(2)–Pd(1)–Cl(2)	89.04(3)
P(2)–Pd(1)–Cl(1)	170.79(8)	P(2)–Pd(1)–Cl(1)	170.59(4)
P(1)–Pd(1)–Cl(2)	173.82(7)	P(1)–Pd(1)–Cl(2)	170.63(4)
Pd(1)–P(1)–C(1)	120.2(2)	Pd(1)–P(1)–C(30)	120.88(13)
Pd(1)–P(1)–C(37)	112.0(2)	Pd(1)–P(1)–C(37)	112.15(13)
Pd(1)–P(1)–C(31)	109.6(3)	Pd(1)–P(1)–C(31)	110.99(13)
C(1)–P(1)–C(37)	101.5(3)	C(30)–P(1)–C(37)	100.39(18)
C(1)–P(1)–C(31)	104.0(3)	C(30)–P(1)–C(31)	101.55(18)
C(31)–P(1)–C(37)	108.6(3)	C(31)–P(1)–C(37)	109.86(18)
Pd(1)–P(2)–C(18)	123.1(2)	Pd(1)–P(2)–C(18)	113.87(13)
Pd(1)–P(2)–C(25)	114.8(3)	Pd(1)–P(2)–C(24)	103.76(13)
Pd(1)–P(2)–C(19)	107.4(2)	Pd(1)–P(2)–C(17)	127.33(13)
C(18)–P(2)–C(19)	102.6(4)	C(18)–P(2)–C(17)	97.76(18)
C(18)–P(2)–C(25)	100.5(3)	C(18)–P(2)–C(24)	107.74(19)
C(19)–P(2)–C(25)	106.9(4)	C(17)–P(2)–C(24)	106.18(18)

expected for palladium complexes of four-carbon tethered diphosphines and are comparable to that reported for [Pd(dppf)Cl_2] [29].

3.3. Catalytic studies

Catalysts formed from a combination of *cis*-11,12-bis(diphenylphosphinomethyl)-9,10-dihydro-9,10-ethano-anthracene (**5a**) and palladium acetate are active for the copolymerization of ethene and carbon monoxide, generating low molecular weight polymers with an activity of 13 300 g polymer (g of Pd)$^{-1}$ h^{-1}. The results of the polymerization experiments and polymer properties are summarized in Table 4. Copolymerization reactions were carried out in methanol under 10 bar each of CO and ethene and after 2 h the reactor was cooled, the polymer isolated by filtration and the reaction mixture analyzed by gas chromatography. The IR spectra of the copolymers (recorded as a KBr disc) contain a CO stretching band at 1692 cm^{-1}. As an example, the $^{13}C\{^1H\}$-NMR spectrum of copolymer generated using *cis*-11,12-bis-(diphenylphosphinomethyl) - 9,10 - dihydro - 9,10 - ethano - anthracene–Pd$(OAc)_2$, recorded in 1,1,1,3,3,3-hexafluoroisopropyl alcohol, contains signals associated with the methylene and carbonyl carbons at δ 35.0 and 212.1 ppm, respectively, and no signals were observed in the region expected for double insertion of C_2H_4 into the polymer [5]. In addition, resonances at δ 217.0 ($CH_3CH_2\mathit{C}O$), 176.4 (MeO*C*O), 6.5 ($\mathit{C}H_3CH_2$), 52.0 ($CH_2O\mathit{C}H_3$) and 27.5 ($\mathit{C}H_2$–C(O)OMe) are clearly visible and correspond to ketone and ester end groups on the polymer. End group analysis of the ^{13}C-NMR spectrum has been used to determine the average degree of polymerization (n) and it has revealed that the polyketone is a short chain polymer with $n = 40$ (Table 4, entry 5).

The formation of polyketone using a catalyst mixture based on **5a** is perhaps not surprising since the majority of diphenylphosphino-substituted phosphines form catalysts that are selective for copolymerization [7,30]. Notably, in his early studies Drent showed a marked dependence of polymer productivity and molecular weight on the length of the tether in the bidentate phosphines $Ph_2P(CH_2)_nPPh_2$ ($n = 1–6$). In particular, he showed that catalysts formed from palladium acetate and 1,3-bis(diphenylphosphino)propane (dppp) gave maximum rates (6000 g polymer (g of Pd)$^{-1}$ h^{-1}) and polymer molecular weights ($n = 180$), whereas those based on a four-carbon tether ($n = 4$, 1,4-bis(-diphenylphosphino)butane) were less active (2300 g polymer (g of Pd)$^{-1}$ h^{-1}) and gave polymer with a significantly lower molecular weight ($n = 45$) [7b]. In order to relate the results obtained using catalyst mixtures formed from **4a**–**b** and **5a**–**b** with those previously reported for dppb, we performed copolymerization reactions using [Pd(dppb)$(OAc)_2$] under our conditions (Table 4, entry 7) and found that the activity and average degree of polymerization compares favorably with catalyst mixtures formed with **5a**. We have not made any attempt to optimize catalyst conditions, either via the use of oxidizing additives such as 1,4-benzoquinone or by varying the Brønsted acid. Rather, we have relied on comparative results obtained using dppb as a standard under our conditions in order to relate the results of our studies to those reported in the literature.

Under similar conditions, catalyst mixtures generated from palladium acetate and *trans*-11,12-bis-(diphenylphosphinomethyl)-9,10-dihydro-9,10-ethano-anthracene (**5b**) produce methyl propanoate (Table 4, entry 6), with an activity of 7300 g methyl propanoate (mol cat)$^{-1}$ hr^{-1} together with polyketone (2,800 g polymer (mol Pd)$^{-1}$ h^{-1}, $n = 20$), giving a selectivity greater than 70%. The selectivity of this catalyst is perhaps not surprising since we have previously shown that the selectivity of catalysts based on *endo*, *exo*- and

Table 4
Summary of ethylene carbon monoxide copolymerization results [a]

Entry	Ligand	Mass of polymer (g) [b]	Productivity/g polyketone (mol cat)$^{-1}$ h^{-1}	n [c]	Mass of propanoate (g) [b,d]	Productivity [d]/g propanoate (mol cat)$^{-1}$ h^{-1}
1	**4a**	3.5	20 600	80	–	-
2	**4b**	1.6	9500	50	–	-
3	**4c**	0	0	–	–	–
4	phosphole [e]	0	0	–	0.20	1200
5	**5a**	2.3	13 300	40	–	–
6	**5b**	0.44	2800	20	1.25	7300
7	dppb	4.5	26 700	45	–	–

[a] All reactions were performed in methanol pressurized to 20 bar with an equimolar mixture of CO–C_2H_4 at 90 °C for 2 h.

[b] Average mass of product over three runs.

[c] The average degree of polymerization (n) estimated by integration of the end group signals in the $^{13}C\{^1H\}$-NMR spectra.

[d] Determined from GC analysis of the reaction mixture using n-decane as an internal standard.

[e] 1-Phenyl-2,3,4,5-tetramethylphosphole.

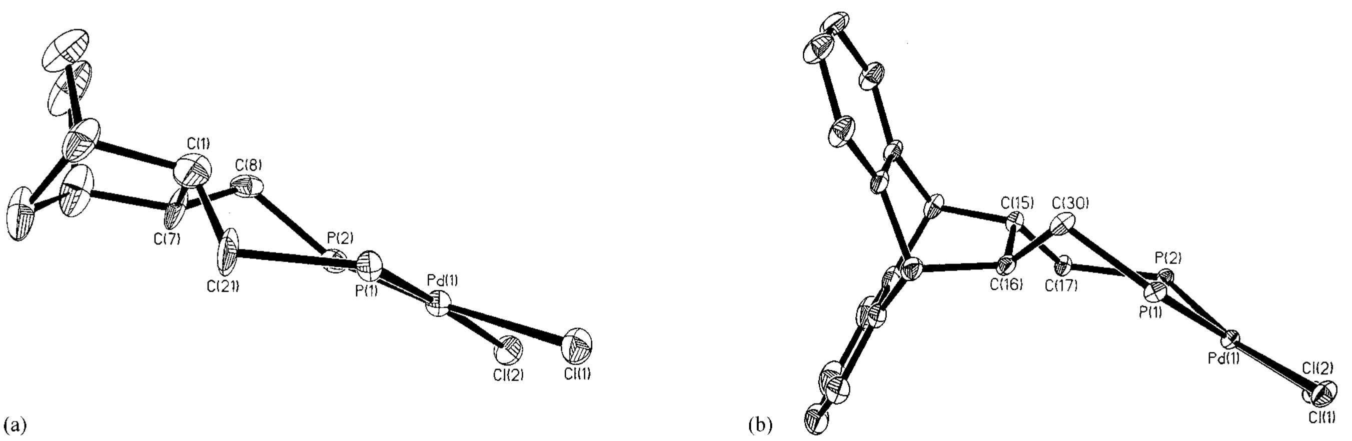

Fig. 5. Perspective views showing the torsional angles in the four-carbon tether of (a) [{*endo*, *exo*-bis(diphenylphosphinomethyl)norbornane}-$PdCl_2$]; (b) [{*trans*-11,12-bis(diphenylphosphinomethyl)-9,10-dihydro-9,10-ethano-anthracene}$PdCl_2$]. Phenyl rings on P(1) and P(2) have been omitted for clarity.

endo, *endo*-bis(diphenylphosphinomethyl)norbornane is strongly influenced by the ligand stereochemistry [13]. Catalysts based on *endo*, *exo*-bis(diphenylphosphinomethyl)norbornane are highly selective for the production of methyl propanoate (> 90%) while those formed from *endo*, *endo*-bis(diphenylphosphinomethyl)norbornane generate polyketone. By analogy, catalysts based on *trans*-11,12-bis(diphenylphosphinomethyl)-9,10-dihydro-9,10-ethano-anthracene, which bears a close stereochemical similarity to *endo*, *exo*-bis(diphenylphosphinomethyl)norbornane in that both contain a conformationally rigid four-carbon tether with a torsional twist about C2–C3, would be predicted to be selective for methyl propanoate. The torsional twist in the four-carbon tethers of [{*trans*-11,12-bis(diphenylphosphinomethyl)-9,10-dihydro-9,10-ethano-anthracene}$PdCl_2$] (torsional ∠C(17)C(15)C(16)–C(30)C(16)C(15) = 76.5°) and [{*endo*, *exo*-bis(diphenylphosphinomethyl)norbornane}$PdCl_2$] (∠C(8)C(7)C(1)–C(21)C(1)C(7) = 76.4°) are shown in Fig. 5, which clearly illustrates the stereochemical similarity between these diphosphines. In contrast, *cis*-11,12-bis(diphenylphosphinomethyl)-9,10-dihydro-9,10-ethano-anthracene more closely resembles *endo*, *endo*-bis(diphenylphosphinomethyl)norbornane in the stereochemical arrangement of the four-carbon tether (torsional angles of 6.4 and 0°, respectively) and, not surprisingly, both form catalysts that are selective for polyketone. In addition to producing methyl propanoate, we noted that catalysts based on *endo*, *exo*-bis(diphenylphosphinomethyl)norbornane also produce polyketone with an average degree of polymerization of 14. If catalyst selectivity results from a large difference in the rate of chain termination versus propagation, the average degree of polymerization would be expected to be significantly less than 14, since methyl propanoate is generated after only a single turnover and thus there would be rapidly diminishing amounts of dimer and higher oligomers. Clearly, the production of polyketone ($n = 14$) and methyl propanoate with > 90% selectivity is not consistent with the presence of a single active catalyst and is most likely due to the presence of two distinct catalytic species operating in parallel, one in which the diphosphine acts in a bidentate manner, to generate polyketone, and the other in which one arm of the diphosphine dissociates and effectively behaves as a monodentate ligand to generate methyl propanoate. Although it is well known that the tendency of bidentate phosphines to open and act as bridging ligands increases with increasing natural bite angle [31], the bite angle of 100.30(1)° associated with [*trans*-11,12-bis(diphenylphosphinomethyl)-9,10-dihydro-9,10-ethano-anthracene}$PdCl_2$] (**6b**) is similar to that formed by *endo*, *endo*-bis(diphenylphosphinomethyl)norbornane, (∠PPdP = 100.53(6)°), which is exclusive for the production of polyketone, during which it presumably acts in a bidentate manner, i.e. if selectivity is determined by monodentate versus bidentate coordination, it is unlikely to depend solely on the natural bite angle but on a subtle combination of factors. Comparison of the structures of **6a**–**d** reveals that the difference in the Pd–P bond lengths in **6d** (ΔPd–P = 0.029 Å) is significantly greater than those in **6a**–**c** (**6a**, 0.0063 Å; **6b**, 0.0008 Å; **6c**, 0.0016 Å) which supports the proposal that *trans*-11,12-bis(diphenylphosphinomethyl)-9,10-dihydro-9,10-ethano-anthracene forms a second distinct catalytic species via dissociation of the less strongly bound diphenylphosphino group. The generation of polyketone and methyl propanoate using *trans*-11,12-bis(diphenylphosphinomethyl)-9,10-dihydro-9,10-ethano-anthracene clearly supports our preliminary observations and the suggestion that the stereochemistry of the four-carbon tether could play a role in influencing catalyst selectivity. Although the average degree of polymerization of 20 for catalysts based on *trans*-11,12-bis(diphenylphosphinomethyl)-

9,10-dihydro-9,10-ethano-anthracene is notably lower than that of its *cis* counterpart ($n = 45$), it is still fully consistent with the presence of two distinct catalytic species.

The dramatic difference in selectivity between catalysts based on 1,2-bis(2,3,4,5-tetramethylphospholylmethyl)benzene and 1,2-bis(di-*tert*-butylphosphinomethyl)benzene, which gave copolymer and methyl propanoate, respectively, prompted us to examine the activity and selectivity of catalysts formed from *cis*- and *trans*-11,12-bis(2,3,4,5-tetramethylphospholylmethyl)-9,10-dihydro-9,10-ethano-anthracene (**4a**–**b**). Under our conditions, catalyst mixtures based on *cis*-11,12-bis(2,3,4,5-tetramethylphospholylmethyl)-9,10-dihydro-9,10-ethano-anthracene and *trans*-11,12-bis(2,3,4,5-tetramethylphospholylmethyl)-9,10-dihydro-9,10-ethanoanthracene gave polyketone with a productivity of 20 000 and 9500 g polymer (mol cat)$^{-1}$ h^{-1}, respectively (Table 4, entries 1 and 2). The copolymer generated using catalysts formed from phospholes **4a** and **b** separated during the reaction as gray, high melting powders (temperature range 250–260 °C). The average degree of polymerization has been estimated by integration of the end group resonances in the solution $^{13}C\{^1H\}$-NMR spectrum. Interestingly, polyketone generated using a catalyst mixture based on **4a** has an unexpectedly high molecular weight ($n = 80$), clearly evident from the exceptionally low intensity of the end group resonances, while polymer generated using **4b** is significantly shorter ($n = 50$) and much closer to the molecular weight of polyketone produced with catalyst based on 1,4-bis(diphenylphosphino)butane [7b].

The most surprising aspect of these studies is the selectivity of *trans*-11,12-bis(2,3,4,5-tetramethylphospholylmethyl)-9,10-dihydro-9,10-ethano-anthracene for copolymerization whereas its diphenylphosphino counterpart gives mainly methyl propanoate. This is consistent with the previous observation in which 1,2-bis(2,3,4,5-tetramethylphospholylmethyl)benzene and 1,2-bis(di-*tert*-butylphosphinomethyl)benzene are selective for copolymer and methyl propanoate, respectively. Such a dramatic change in selectivity for bidentate ligands may be due to steric protection of the axial sites offered by the phospholyl groups, which prevents chain termination via an associative process. In addition, the phospholyl fragment resembles 1,10-phenanthroline and 2,2-bipyridine, which form catalysts that are selective for copolymerization, in that they provide limited effective shielding of the active sites *trans* to the bidentate ligand. However, if, as suggested earlier, *trans*-11,12-bis(diphenylphosphinomethyl)-9,10-dihydro-9,10-ethano-anthracene forms two active species, one in which the phosphine acts in a monodentate manner the other as a bidentate ligand, it is difficult to understand why *trans*-11,12-bis(2,3,4,5-tetramethylphospholylmethyl)-9,10-dihydro-9,10-ethano-anthracene does not behave in a similar manner and generate methyl propanoate. Further studies are clearly required to establish the origin of this selectivity.

To evaluate the effect of the phosphole substitutent, in combination with a four-carbon tether, [{1,4-bis(2,3,4,5-tetramethylphospholyl)butane}Pd(OAc)$_2$] was prepared and used to catalyze the copolymerization of C_2H_4 and CO. In a comparative experiment, under the same conditions as those used with **5a** and **b**, catalysts generated from 1,4-bis(2,3,4,5-tetramethylphospholyl)butane are inactive for either copolymerization or methoxycarbonylation (Table 4, entry 3), which appears to be due to catalyst instability, as evidenced by the rapid formation of a dark colored precipitate characteristic of decomposition. The poor performance of 1,4-bis(2,3,4,5-tetramethylphospholyl)butane contrasts sharply with the high activity of catalysts based on dppb and further highlights the marked influence of the nature of the substituents attached to phosphorus in determining catalyst activity/stability. However, spectroscopic studies have shown that 1,4-bis(2,3,4,5-tetramethylphospholyl)butane does not act in a bidentate manner but most likely bridges two metal centers to form polymers/oligomers (vide infra), a factor which will also influence catalyst performance. In addition, comparison of the performance of catalysts based on *trans*-11,12-bis(diphenylphosphinomethyl)-9,10-dihydro-9,10-ethano-anthracene and *trans*-11,12-bis-(2,3,4,5-tetramethylphospholyl)-9,10-dihydro-9,10-ethano-anthracene further reinforces the idea that, for diphosphines that act as bidentate ligands, selectivity is influenced by the substituents attached to phosphorus.

The key discovery in polyketone chemistry involving replacement of the monodentate phosphine PPh_3 for the chelating bidentate dppp which resulted in a change in selectivity from methyl propanoate to polyketone prompted us to investigate the dependence of catalyst selectivity on ligand denticity, by conducting catalyst testing using a combination of palladium acetate and the monodentate phosphole 1-phenyl-2,3,4,5-tetramethylphosphole. Under the same conditions as those used for **4a** and **b** and **5a** and **b**, catalysts based on monodentate phospholes are inactive for copolymerization and show only low activity for alkoxycarbonylation (Table 4, entry 4), confirming the observation that monodentate ligands do not form catalysts that are selective for polyketone.

In conclusion, following our preliminary studies in which we demonstrated that catalyst systems based on the C_4-bridged diphosphine *endo*, *endo*-2,3-bis-(diphenylphosphinomethyl)norbornane are selective for copolymerization of ethylene with carbon monoxide while those formed from its *exo*, *endo*-2,3-bis-(diphenylphosphinomethyl)norbornane counterpart are highly selective for the production of methyl propanoate, we have now shown that catalysts based on *cis*- and *trans*-11,12-bis(diphenylphosphinomethyl)-9,10-dihydro-9,10-ethano-anthracene show similar selectivity patterns. Single-crystal X-ray structure determinations have revealed only minor differences in the bite angles of these phosphines and clearly selectivity must be determined by a combination of factors, one of which appears to be the stereochemistry of the C_4-tether. Substitution of the diphenylphosphino groups in *trans*-11,12-bis(diphenylphosphinomethyl)-9,10-dihydro-9,10-ethano-anthracene for the 2,3,4,5-tetramethylphospholyl fragment results in a dramatic reversal of selectivity and catalysts based on *trans*-11,12-bis(2,3,4,5-tetramethylphospholyl)-9,10-dihydro-9,10-ethano-anthracene are selective for the production of polyketone. In the case of phosphole-based catalysts, the nature of the four-carbon tether appears to play an important role in determining stability since catalysts formed from 1,4-bis(2,3,4,5-tetramethylphospholyl)-butane decompose rapidly under conditions of copolymerization. Clearly, evaluation of the factors that influence catalyst selectivity, activity and polymer molecular weight is not straightforward and further studies are required to fully investigate the origin of these effects. In particular, investigations into counterion effects, the preparation of cationic methyl and methoxycarbonyl precatalysts and variations in the electronic and steric properties of the phospholyl fragment are currently under way.

4. Supplementary material

Crystallographic data for the structural analysis have been deposited with the Cambridge Crystallographic Data Centre, CCDC nos. 116121, 116122, 116123, and 116124 for compounds **6d**, **6c**, **6b and 6a**, respectively. Copies of this information may be obtained free of charge from The Director, CCDC, 12 Union Road, Cambridge CB2 1EZ, UK (Fax: +44-1223-336033; e-mail: deposit@ccdc.cam.ac.uk or www: http://www.ccdc.cam.ac.uk).

Acknowledgements

We gratefully acknowledge funding from the University of Newcastle upon Tyne, EPSRC (E.G.R., P.A.C., equipment to W.C.) and INEOS Acrylics (P.A.C.), and thank Johnson Matthey for loans of palladium salts.

References

[1] J. Tsuji, Palladium Reagents and Catalysts. Innovations in Organic Synthesis, Wiley, New York, 1995.

[2] (a) C.G. Chardarin, S.L. Wov, R.C. Clark, C.H. Hathcock, Tetrahedron Lett. (1976) 1769;
(b) T.F. Murray, E.G. Samsel, V. Varma, J.R. Norton, J. Am. Chem. Soc. 193 (1981) 7520;
(c) T.F. Murray, V. Varma, J.R. Norton, J. Org. Chem. 43 (1978) 353;
(d) B. El Ali, H. Alper, J. Org. Chem. 56 (1991) 5357.

[3] H. Alper, N. Hamel, J. Am. Chem. Soc. 112 (1990) 2803.

[4] (a) S.E. Houssame, L.E. Firdoussi, S. Allaoud, A. Karim, Y. Castanet, A. Mortreux, J. Mol. Catal. A. 168 (2001) 15;
(b) L.E. Firdoussi, A. Bagga, S. Allaoud, B. Ait Allal, A. Karim, Y. Castanet, A. Mortreux, J. Mol. Catal. A. 135 (1998) 11.

[5] (a) E. Drent, P.H.M. Budzelaar, Chem. Rev. 96 (1996) 663;
(b) A. Sen, Acc. Chem. Res. 26 (1993) 303;
(c) K. Nozaki, T. Hiyama, J. Organomet. Chem. 576 (1999) 248;
(d) B. Milani, G. Mestroni, Comments Inorg. Chem. 20 (1999) 301;
(e) M. Sperrle, G. Consiglio, Chem. Ber. 130 (1997) 1557;
(f) A. Vavasori, L. Toniolo, J. Mol. Catal. A 110 (1996) 13;
(g) E. Drent, J.A.M. van Broekhoven, P.H.M. Budzelaar, in: B. Cornils, W.A. Hermann (Eds.), Applied Homogeneneous Catalysis with Organometallic Compounds, vol. 1, VCH, Weinheim, 1996 (333 pp.).

[6] (a) E. Drent, Eur. Patent Appl., EP 0 495 548 (1992);;
(b) E. Drent, Eur. Patent Appl., EP 0 495 547 (1992);;
(c) E. Drent, Eur. Patent Appl., WO 97/03943 (1997);;
(d) G.R. Eastham, R.P. Tooze, X.L. Wang, K. Whiston, (ICI) WO 96/19434 (1996);;
(e) G.W. Parshall, S.D. Ittel, Homogeneous Catalysis: The Applications and Catalysis by Soluble Transition Metal Complexes, Wiley, New York, 1992.

[7] For examples of diphosphines see: (a) E. Drent, Eur. Pat. Appl. 121 965 A2, 1984;
(b) E. Drent, J.A.M. van Broekhoven, M.J. Doyle, J. Organomet. Chem. 417 (1991) 235;
(c) M. Barsacchi, A. Batistini, G. Consiglio, U.W. Suter, Macromolecules 25 (1992) 3604;
(d) M. Sperrles, G. Consiglio, J. Am. Chem. Soc. 117 (1995) 12130;
(e) Z. Jiang, S.E. Adams, A. Sen, Macromolecules 27 (1994) 2694;
(f) Z. Jiang, A. Sen, J. Am. Chem. Soc. 117 (1995) 4455;
(g) C. Bianchini, H.M. Lee, A. Meli, S. Moneti, F. Vizza, M. Fontani, P. Zanello, Macromolecules 32 (1999) 4183;
(h) C. Bianchini, H.M. Lee, A. Meli, W. Oberhauser, F. Vizza, P. Bruggeller, R. Haid, C. Langes, Chem. Commun. (2000) 777;
(i) G. Verspini, F. Schanserra, R.A. Sheldon, Angew. Chem. Int. Ed. Engl. 39 (2000) 803;
For examples of dintrogen donors see: (j) F.C. Rix, M. Brookhart, P.S. White, J. Am. Chem. Soc. 118 (1996) 4746;
(k) B. Milani, A. Anzilutti, L. Vicentini, A. Sessanta Santi, E. Zangrando, S. Geremia, G. Mestroni, Organometallics 16 (1997) 5064;
(l) B.A. Markies, D. Kruis, M.H.P. Rietveld, K.A.N. Verberk, J. Boersma, H. Koojima, M.T. Lakin, A.L. Speck, G. van Koten, J. Am. Chem. Soc. 117 (1995) 117, 5263;
(m) M. Brookhart, F.C. Rix, J.M. DeSimone, J.C. Barborak, J. Am. Chem. Soc. 114 (1992) 5894;
(n) M. Brookhart, M.I. Wagner, G.G.A. Balavoine, H.A. Haddou, J. Am. Chem. Soc. 1126 (1994) 3641;
(o) B. Milani, L. Vicentini, A. Sonmazzi, F. Garbassi, E. Chiarparin, E. Zangrando, G. Mestroni, J. Chem. Soc. Dalton Trans. (1996) 3139;
(p) B. Milani, E. Alessio, G. Mestroni, E. Zangrando, L. Randaccio, G. Consiglio, J. Chem. Soc. Dalton Trans. (1996) 1021;
(q) M. Brookhart, M.I. Wagner, J. Am. Chem. Soc. 118 (1996) 7219;

(r) L.K. Johnson, S. Mecking, M. Brookhart, J. Am. Chem. Soc. 118 (1996) 267.

[8] W. Clegg, G.R. Eastham, M.R.J. Elsegood, R.P. Tooze, X.L. Wang, K. Whiston, Chem. Commun. (1999) 1877.

[9] G.R. Eastham, B.T. Heaton, J.A. Iggo, R.P. Tooze, R. Whyman, S. Zucchini, Chem. Commun. (2000) 609.

[10] R.P. Tooze, K. Whiston, A.P. Malyan, M.J. Taylor, N.W. Wilson, J. Chem. Soc. Dalton Trans (2000) 3441.

[11] A. Seayad, S. Jayasree, K. Damodarao, L. Toniolo, R.V. Chaudhari, J. Organomet. Chem. 601 (2001) 100.

[12] S. Doherty, G.R. Eastham, R.P. Tooze, T.S. Scanlan, D. Williams, M.R.J. Elsegood, W. Clegg, Organometallics 18 (1999) 3558.

[13] J.G. Knight, S. Doherty, A. Harriman, E.G. Robins, M. Betham, G.R. Eastham, R.P. Tooze, M.R.J. Elsegood, P. Champkin, W. Clegg, Organometallics 19 (2000) 4957.

[14] K. Weinges, W. Sipos, J. Klein, J. Deuter, H. Irngartinger, Chem. Ber. 120 (1987) 5.

[15] P.J. Fagan, W.A. Nugent, J.C. Calabrese, J. Am. Chem. Soc. 116 (1994) 1880.

[16] G.M. Sheldrick, SHELXTL User Manual, Version 5, Bruker AXS Inc, Madison, WI, 1994.

[17] SMART and SAINT software for CCD diffractometers, Bruker AXS Inc., Madison, WI, 1994.

[18] P. Gradoz, D. Baudry, M. Ephritikhine, F. Nief, F. Mathey, J. Chem. Soc. Dalton Trans. (1992) 3047.

[19] J.J. MacDougall, J.H. Nelson, F. Mathey, J. Mayerle, J. Inorg. Chem. 19 (1980) 709.

[20] T.A. Stephenson, S.M. Morehouse, A.R. Powell, J.P. Heffer, G. Wilkinson, J. Chem. Soc. (1965) 3632.

[21] M. Gougygou, O. Tissot, J.-C. Daran, G.G.A. Balavoine, Organometallics 16 (1997) 1008.

[22] J.J. MacDougall, J.H. Nelson, F. Mathey, J.J. Mayerle, Inorg. Chem. 19 (1980) 709.

[23] T. Kojima, K. Saeki, K. Ono, M. Ohba, Y. Matsuda, Chem. Commun. (1997) 1697.

[24] W.L. Wilson, J. Fischer, R.E. Wasylishen, K. Eichele, V.J. Catalano, J.H. Frederick, J.H. Nelson, Inorg. Chem. 35 (1996) 1486.

[25] N. Gul, J.H. Nelson, Tetrahedron 26 (2000) 71.

[26] N. Gul, J.H. Nelson, Organometallics 19 (2000) 91.

[27] V.D. Makhaev, Z.M. Dzhabieva, S.V. Konovalikhin, O.A. D'Yachenko, G.P. Belov, Koord. Khim. 22 (1996) 598.

[28] V. Gramlich, G. Consiglio, Helv. Chim. Acta 62 (1979) 1016.

[29] T. Hayashi, M. Konishi, Y. Kabori, M. Kumada, T. Higuchi, K. Mirotsu, J. Am. Chem. Soc. 106 (1984) 158.

[30] (a) S.J. Dossett, A. Gillon, A.G. Orpen, J.S. Fleming, P.G. Pringle, D.F. Wass, M.D. Jones, Chem. Commun. (2001) 699;
(b) G.K. Barlow, J.D. Boyle, N.A. Cooley, T. Ghaffar, D.F. Wass, Organometallics 19 (2000) 1470.

[31] (a) P. Dierkes, P.W.M.N. van Leeuwen, J. Chem. Soc. Dalton Trans. (1999) 1519;
(b) A.R. Sanger, J. Chem. Soc. Dalton Trans. (1977) 1971;
(c) G. Consiglio, C.A.S. Nefkens, Tetrahedron: Asymmetry 1 (1990) 417;
(d) M. Portnoy, Y. Ben-David, D. Milstein, J. Organomet. Chem. 503 (1995) 149;
(e) G.P.C.M. Dekker, C.J. Elsevier, K. Vrieze, P.W.M.N. van Leeuwen, Organometallics 11 (1992) 1598;
(f) N.A. Al-Salem, H.D. Empsall, R. Markham, B.L. Shaw, B. Weeks, J. Chem. Soc. Dalton Trans. (1979) 1972.